ELSEVIER

Biochimica et Biophysica Acta 1564 (2002) 21–30

BIOCHIMICA ET BIOPHYSICA ACTA
BBA

www.bba-direct.com

Ultradeformable lipid vesicles can penetrate the skin and other semi-permeable barriers unfragmented. Evidence from double label CLSM experiments and direct size measurements

Gregor Cevc [a,*], Andreas Schätzlein [a,b], Holger Richardsen [b]

[a] *Medizinische Biophysik, Technische Universität München, Ismaningerstr 22, D-81675 Munich, Germany*
[b] *IDEA AG, Frankfurter Ring 193a, D-80807 Munich, Germany*

Received 18 September 2001; received in revised form 1 February 2002; accepted 21 March 2002

Abstract

The stability of various aggregates in the form of lipid bilayer vesicles was tested by three different methods before and after crossing different semi-permeable barriers. First, polymer membranes with pores significantly smaller than the average aggregate diameter were used as the skin barrier model; dynamic light scattering was employed to monitor vesicle size changes after barrier passage for several lipid mixtures with different bilayer elasticities. This revealed that vesicles must adapt their size and/or shape, dependent on bilayer stability and elasto-mechanics, to overcome an otherwise confining pore. For the mixed lipid aggregates with highly flexible bilayers (Transfersomes®), the change is transient and only involves vesicle shape and volume adaptation. The constancy of ultradeformable vesicle size before and after pores penetration proves this. This is remarkable in light of the very strong aggregate deformation during an enforced barrier passage. Simple phosphatidylcholine vesicles, with less flexible bilayers, lack such capability and stability. Conventional liposomes are therefore fractured during transport through a semi-permeable barrier; as reported by other researchers, liposomes are fragmented to the size of a narrow pore if sufficient pressure is applied across the barrier; otherwise, liposomes clog the pores. The precise outcome depends on trans-barrier flux and/or on relative vesicle vs. pore size. Lipid vesicles applied on the skin behave accordingly. Mixed lipid vesicles penetrate the skin if they are sufficiently deformable. If this is the case, they cross inter-cellular constrictions in the organ without significant composition or size modification. To prove this, we labelled vesicles with two different fluorescent markers and applied the suspension on intact murine skin without occlusion. The confocal laser scanning microscopy (CLSM) of the skin then revealed a practically indistinguishable distribution of both labels in the stratum corneum, corroborating the first assumption. To confirm the second postulate, we compared vesicle size in the starting suspension and in the blood after non-invasive transcutaneous aggregate delivery. Size exclusion chromatograms of sera from the mice that received ultradeformable vesicles on the skin were undistinguishable from the results measured with the original vesicle suspension. Taken together, the results support our previous postulate that ultradeformable vesicles penetrate the skin intact, that is, without permanent disintegration. © 2002 Published by Elsevier Science B.V.

Keywords: Vesicle stability; Bilayer elasticity; Aggregate deformability; Skin barrier penetration; Transdermal drug delivery; Confocal laser scanning microscopy; Size exclusion; Transfersomes®

1. Introduction

First description of epicutaneous application of liposomes is more than 20 years old [1,2]. Since then, close to a thousand papers have been published on the use of vesicles comprising non-ionic surfactants [3,4], synthetic or chemically modified lipids, plant lipids [5,6] or skin lipids [7,8], but also lipid–surfactant combinations [9] on the skin. In some studies, skin permeation enhancers were included [1,2]; in other cases, additional gadgets, such as iontophoresors [10], were employed to improve the efficacy of transdermal delivery of lipid vesicles.

Phospholipid vesicle suspensions (liposomes) are contained in five marketed topical therapeutics [11] and at least nominally in countless cosmetic formulations [12]. This is a remarkably optimistic practice in light of the huge discrepancy between a typical liposome size and the width of the natural passage through the skin: even small unilamellar liposomes are rarely smaller than 50 nm [13] unless they are

* Corresponding author. Tel.: +49-89-324-63310; fax: +49-89-324-1684.
E-mail address: Cevc@idea-ag.de (G. Cevc).

0005-2736/02/$ - see front matter © 2002 Published by Elsevier Science B.V.
PII: S0005-2736(02)00401-7

unreasonably (e.g. ultrasonically) stressed, and/or supplemented with surfactants or degradation products. In contrast, pores in the skin are normally 0.3 nm narrow [14] and can be opened without major skin damage merely to 20–40 nm at most [14,15]. It is therefore difficult to contemplate how an entire liposome could cross the skin and participate in its entirety in transdermal transport.

Many researchers consequently believe that phospholipids administered on the skin as aggregates first disintegrate and then diffuse through the barrier in the form of small fragments or lipid monomers [16–18]; this probably happens to lipid aggregates below the skin surface. At the skin surface, simple phospholipid vesicles were reported to break down or to fuse [16,19,20]. Liposomes made from sufficiently hydrophilic lipids then may promote material diffusion through the barrier by increasing the skin hydration [21].

Most lipid vesicles are typically retained on or break in a semi-permeable barrier with openings significantly smaller than the average vesicle diameter; pushing lipid suspension through the cylindrical pores in a polycarbonate membrane is therefore popular for downsizing conventional liposomes. The method was introduced by the group of the late D. Papahadjopoulos [22] and is now often used for manufacturing liposomes as drug carriers [23–27].

Extrusion of a lipid suspension through 100 nm pores yields vesicles of approximately (140 ± 40) nm diameter [23]; wider or narrower pores typically yield correspondingly greater or smaller vesicle/pore size ratios [24,28]. Final vesicle size normally falls in the range $r_{\mathrm{pore}}\ 1 \simeq \cdots 1.5\ r_{\mathrm{pore}}$ [28]. Narrower pores yield higher relative vesicle diameters in the range and vice versa. Repeated extrusion also reduces the number of lipid lamellae per vesicle [25] and brings the final vesicle size closer to the employed pore diameter [28].

Two essential requirements must be fulfilled for a successful extrusion of conventional liposomes through a microporous barrier: sufficient lipid bilayer fluidity [26] and the use of extrusion pressure greater than certain, lipid-dependent lower limit [27]. This limit increases linearly with the inverse pore size, as suggested by Young's equation [27]. However, pore sizes around or below 30 nm require exceptionally high pressures in excess of 2 MPa [27]. They also yield anomalously stressed, and relatively large, final vesicles.

The question of liposome passage through the skin is closely related, but not identical, to the problem of vesicle transport through artificial barriers. For example, with the experience gained in liposomes extrusion studies, one cannot explain why small lipid aggregates or solubilised lipids fail to permeate through the skin better than plain vesicles. The fact that mixed lipid vesicles with a highly flexible/fluid membranes are better skin penetrants than the much smaller mixed lipid micelles [15,29,30] also awaits generally accepted explanation.

We advocate a differentiated concept of lipid aggregate transport through the skin. We agree that simple liposomes do not overcome the barrier intact. We argue, however, that complex aggregates with a more flexible membrane, so-called Transfersomes®[1] [31,15], can cross the skin without irreversible disruption. This is due mainly to the fact that such complex aggregates are at least one order of magnitude more elastic, and thus more deformable, than simple lipid liposomes.

To interpret the motion of suitably designed, ultradeformable vesicles across the stratum corneum and other less complex barriers, we introduced a self-consistent theoretical model [31,32]. This focuses on aggregate deformability and on the existence of an aggregate independent trans-barrier gradient are the two most important factors for successful passage through a semi-permeable barrier [31]. The most obvious natural transdermal gradient originates from water activity difference across the stratum corneum [33]. This gradient acts simultaneously on all vesicle ingredients. Transdermal hydration difference therefore creates a very strong force acting on the skin via vesicles. This enforces widening of the weakest intercellular junctions in the barrier and creates 20–30-nm-wide transcutaneous channels [34]. The channels allow sufficiently deformed, slimed lipid vesicles to cross the skin along the said hydration gradient. Spontaneous motion of the highly deformed, hydrophilic entities through the skin barrier is consequently based on barrier penetration rather than on trans-barrier permeation.[2] It is therefore inappropriate to apply the rules of diffusion to vesicle transport across the skin!

To date, Transfersomes® were used to deliver numerous small chemical entities [30,35] and relatively large therapeutics [11,36], but also proteins [37,38] across the skin. This was done in preclinical experiments using mice, rats, and pigs as test animals, and also in phase I and phase II clinical studies. A total of 10 clinical investigations were successfully completed to date. The ability of Transfersomes® to deliver drugs across the skin is therefore well-documented and widely accepted. It could not be clarified, though, whether ultradeformable vesicles can overcome the skin barrier without fragmentation, that is, physically intact.

In this publication, we addressed the problem of exogenous lipid vesicle detection by combining the results of three pertinent experimental techniques. For this purpose, we first used the dynamic light scattering on vesicle suspension; this demonstrated that the passage of large ultradeformable vesicles through a nanoporous membrane can, but need not, be completely non-destructive. Secondly, we studied the transport of similar fluorescently labelled vesicles through the stratum corneum by means of the confocal laser scanning microscopy (CLSM). This

[1] Transfersome® is a trademark of IDEA AG.

[2] In the context of this work, we use the word 'permeation' to describe a diffusive trans-barrier flow of individual molecules and the word 'penetration' to outline a concentration-independent motion of aggregates through nanoporous barriers.

revealed that various labels co-penetrate into murine skin, we thus confirmed indirectly the maintenance of Transfersome® composition during the process. Last but not least, we recovered labelled aggregates from the systemic blood circulation of the mice that were treated epicutaneously with Transfersomes®. Size-exclusion chromatography then allowed us to conclude that the recovered vesicle size is indistinguishable from the size in original suspension. All data taken together provide a rather compelling evidence for vesicle integrity during and after crossing a nanoporous barrier, confirming our initial assumption.

2. Materials and methods

2.1. Lipid suspensions

Lipid suspensions were prepared by mixing ingredients in an organic solvent ($CHCl_3/CH_3OH$ 1:1 v/v). The solution was deposited on walls of a glass vessel and dried under vacuum (≤ 10 Pa; ≥ 12 h). The resulting thin lipid film was hydrated with a buffer (pH = 7.2) to create a suspension (10 wt.% total lipid), which was homogenized further by sonication (titanium micro-tip, Heat Systems W 380, USA, 30 min, 4 °C). Alternatively, we used a sequential—and in some cases repeated—filtration through a nanoporous filter [24] of the appropriate size (i.e., 400, 200, 100, 80 nm) to the same effect. Vesicle size was measured at different stages by the dynamic light scattering (ALV-5000 correlator, ALV-Laser Vertriebsgesellschaft, Langen, Germany; 90°) under standard conditions (21 °C; 0.2 wt.% total lipid). The final value was typically 150 ± 30 nm, unless stated otherwise.

For microscopy and size-exclusion chromatography, Transfersomes® were co-labelled with 0.2 mol% to 1.5 mol% rhodamine-DHPE (Lissamine™ rhodamine B 1,2-dihexadecanoyl-*sn*-glycero-3-phosphoethanolamine, triethylammonium salt; Ex/Em: 560/581), Texas Red-DHPE (Texas Red™ 1,2-dihexadecanoyl-*sn*-glycero-3-phosphoethanolamine, triethylammonium salt; Ex/Em: 583/601) or with fluorescein-DHPE (*N*-(fluorescein-5-thiocarbamoyl-1,2-dihexadecanoyl-*sn*-glycero-3-phosphoethanolamine, triethylammonium salt; Ex/Em: 496/519), all from Molecular Probes, Eugene, OR, USA). Characteristic wavelengths were sufficiently different to allow adequate differentiation between the used labels. To minimise the danger of false-positive observations, both labels were chosen to have a molecular weight significantly higher (1183 for Fl-PE and 1334 for Rh-PE) than the molecular weight cut-off for the corresponding monomer diffusion across the skin [39].

The labels were mixed with the lipids in an organic solvent. Label co-incorporation into lipid bilayers was essentially quantitative (see Fig. 1 for illustration) due to the covalent fluorophore attachment to vesicle bilayers via a hydrophobic anchor. In spite of this, one would expect to detect bilayer composition changes, as reflected in fluorescence intensity changes, in case of differential label partitioning into the surrounding. Such re-partitioning is not unlikely after vesicle fragmentation, taken that the two fluorophores have distinct chemical nature, polarity, size, and charge. The latter, which is pH sensitive for Fl-PE in the skin relevant range ($pK \sim 6.2$) is particularly likely to cause said fluorescence deviations.

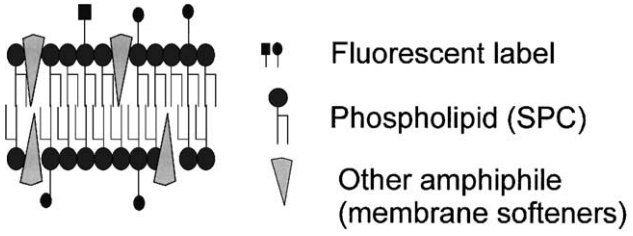

Fig. 1. Schematic representation of a lipid bilayer labelled with two different lipophilic fluorescent dies (Rh-PE, Fl-PE).

To obtain deformable vesicles, we increased lipid bilayer flexibility by adding suitable membrane softening agents into suspension. 'Type C' Transfersomes® were formed from 89 wt.% phosphatidylcholine (ex soya, 98% pure; Nattermann Phospholipids, Cologne, Germany) and 11 wt.% sodium cholate (p.a.; Merck, Darmstadt, Germany); bio-compatible non-ionic surfactants were used in an appropriate relative concentration to produce the 'type T' suspensions.

2.2. Vesicle transport through an artificial membrane

A nanoporous barrier was used to simulate the skin barrier. It was chosen to have a high density of constant size pores and was placed in a custom-made device, similar to the commercially available stainless steel pressure filter holders (Sartorius, Göttingen, Germany). This allowed reproducible measurements of the trans-barrier flow that was driven by an external hydrostatic pressure. Typically, up to 18 ml of the test suspension were pushed through a barrier with pores of 20 nm diameter under the pressure of up to 1 MPa. Only occasionally larger pore sizes (up to 50 nm) were used. The resulting flux, J, was monitored gravimetrically by a remotely controlled analytic balance (Sartorius). Vesicle radius, r_v, before and after barrier passage was measured by the dynamic light scattering (ALV, Langen, Germany).

2.3. Animal experiments

Nude mice (balb/c, nu/nu; age 8–12 weeks) were kept under standard laboratory conditions (three to five per suspending cage; standard diet; water, ad libitum; 12 h light/dark regime). The test suspensions (10–25 μl) were administered to a standardized area on the upper back under mild general anaesthesia (ketamin/xylazin mixture). Ani-

mals were kept on a heating pad during the sedation period (30–45 min) and were transferred into cages (one animal/cage) after recovery.

Excess water from the test suspension typically evaporated in approximately 30 min; a macroscopically dry lipid film, believed to contain highly concentrated vesicles suspension, was left behind. Eight to twelve hours after epicutaneous administration of lipid vesicles (for chromatographic or CLSM experiments, respectively) the study animals were killed by heart puncture. The residual suspension was removed from the skin with a cotton swab. The treated skin was then separated from the underlying tissue. Careful excision yielded 0.5–1 cm^2 samples that were used for microscopic examination (see Ref. [34] for details).

2.4. Confocal laser scanning microscopy (CLSM)

The LSM 410 invert confocal microscope (Zeiss, Jena, Germany) with high numeric aperture lenses (Plan-Neofluar oil immersion lenses: 40/1.3, 63/1.4, 100/1.3) and a minimised pinhole size ($\leq 10\%$ of maximum) was used for the image acquisition at a maximum pixel resolution (1024×1024) (more detailed information is given in Ref. [34]). The 488 nm and 543 nm laser lines were used to excite fluorescein and rhodamine labels, respectively. (The focal depth is a function of pinhole size and of the excitation light wavelength. Pinhole size was therefore optimised separately for each wavelength, and the focal depth consequently differed slightly for each label. A focal depth-based correction would probably have improved probe co-localisation but would also have been impractical).

Images (320×320 μm^2) were taken consecutively with the optimised dichroitic beam splitters and filters to minimise channel cross-talk. All images were acquired with identical settings. The photomultiplier gain/sensitivity/contrast was adjusted to give a slightly over-modulated signal scaling in the fast scan mode. Frame averaging resulted in gray scale images with an optimised final dynamic range. All images were processed with the software packages AVS 5.1 (Advanced Visualizations System Inc., Waltham, MA, USA), IDL 3.9 (Research Systems Inc., Boulder, CO, USA) and Origin 5.0 (Microcal, Northhampton, MA, USA), which were also used for the calculation of the two-dimensional correlation functions.

2.5. Size exclusion chromatography

The HPLC system consisted of a quaternary pump P4000, autosampler AS3500, and a fluorescence detector FL 3000 (all from Thermoseparation Products, Hanau, Germany). A refractive index detector (ERC 7512, ERC Inc., Tokyo, Japan) was used as well. The mobile phase (pH = 6.8) contained 0.5 M Na_2HPO_4/NaH_2PO_4, 0.15 M NaCl and 0.1 mM NaN_3.

The BioRad SEC columns SEC4000 and SEC6000 were used in a series to increase resolution. For quality controls, a series of globular proteins (GFC standard 151-1901, Bio-Rad, München, Germany) was used, and a suspension of well-defined, monodisperse vesicles with the known diameter was measured with the dynamic light scattering. For each data point determination, 5–10 μl of undiluted serum were injected and analysed using a flow rate of 0.5–1.5 ml min^{-1} at 30 °C.

3. Results

The aim of our study was to investigate the passage of ultradeformable vesicles through nanoporous barriers, mimicking or obtained from the skin, with regard to aggregate fragmentation or disintegration.

Previous studies [15] have shown that bilayer elasticity is governing factor for vesicle transport through the skin. The other factor is the force/pressure exerted on the skin by an aggregate. If this force is strong enough, we postulated it can open channels in the barrier up to the size of the deformed vesicle. The process depends on vesicle size before and in the pore, and therefore on vesicle integrity during barrier crossing.

Transfersomes® differ from more conventional lipid aggregates in several respects. The most important is the extremely high and stress-dependent adaptability of such mixed lipid aggregates. Said aggregates are thus ultradeformable and can squeeze themselves between the cells in the stratum corneum, despite the large average vesicle size. The provisos are high membrane elasticity and permeability, sufficient vesicle stability, and a large enough trans-barrier water activity gradient. (The central role of hydrotaxis in transcutaneous transport explains why the skin occlusion normally lowers the rate of transcutaneous lipid vesicle transfer despite the fact that it increases the rate of concentration-driven molecular permeation across the skin).

Vesicle deformation in a confining pore can be expressed in terms of an elongation factor. This is obtained by dividing the length of a spherically-caped, cylindrically deformed vesicle in a pore with the diameter of an assumedly spherical vesicle outside the pore. The purely geometrical result is given in relative units in Fig. 2. This shows that a vesicle three times greater than the pore diameter has to grow by more than this factor in length inside a pore. This creates a rather unfavourable thickness–length ratio.

An elongation ratio of 3.3:1 would be required for a small, unilamellar 60 nm vesicle if this aggregate were to enter a 20 nm pore in the skin; for a 120 nm vesicle the factor is 6.6:1. Obviously, deformations of this magnitude are not achievable with pure phosphatidylcholine liposomes: such vesicles are fractured only with great difficulty to the size of 40 nm [40] and typically have a diameter greater than 60 nm [24] or greater than 100 nm [41].

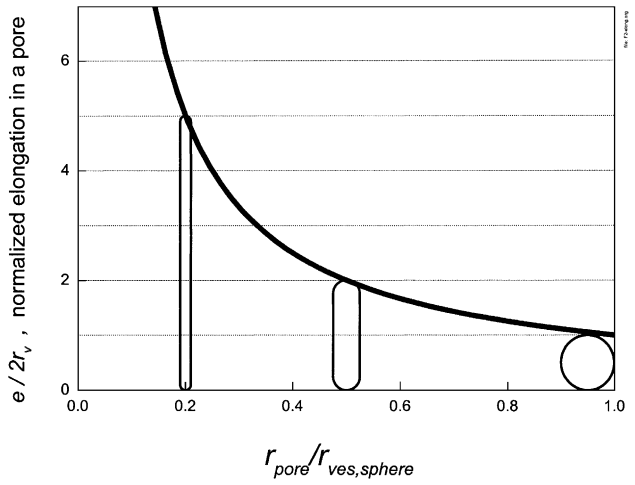

Fig. 2. Normalised vesicle elongation relative to original spherical vesicle size (r_{ves}) as a function of the pore radius (r_{pore}) in a semi-permeable barrier crossed by a vesicle. To the left of the vertical dashed line, vesicle volume reduction is a must.

The energy cost for vesicle elongation in a pore must be paid by an external potential that drives vesicles into its constriction; the trans-barrier water activity gradient, known to exist in the outermost skin region, is normally responsible for this.

3.1. Penetration of an artificial membrane

In order to study in detail the transport of vesicles through the skin-mimicking, semi-permeable barrier, we developed an in vitro model. This model relies on measuring the flux (f) of vesicle suspension across a nanoporous barrier as a function of trans-barrier *pressure gradient* [15,42].

When exposed to a driving pressure around 1 MPa, ultradeformable vesicles cross pores that are much smaller than the average vesicle diameter nearly as rapidly as a buffer of comparable viscosity. This implies that their lipid bilayer adapts to the stress-induced vesicle deformation. We described this in greater detail in previous publications [15,31,36]. This notwithstanding, it is also worthwhile to investigate whether or not the mixed lipid vesicles with a highly flexible membrane can penetrate a nanoporous barrier above the transport-enabling pressure limit without getting broken down. To check for this, we compared the average aggregate size before and after pore passage at various flow rates (see Fig. 3).

The high adaptability of certain vesicles allow such aggregate to maintain sizes much larger than the pore diameter even after trans-barrier transport. This is tantamount to saying that the consumed energy of a pore crossing is used mainly for reversible vesicle deformation and friction and not for major vesicle size diminution. In contrast, liposomes essentially take the size of pores, within experimental uncertainty limits, unless they approach a lower size limit of approximately 60 nm.

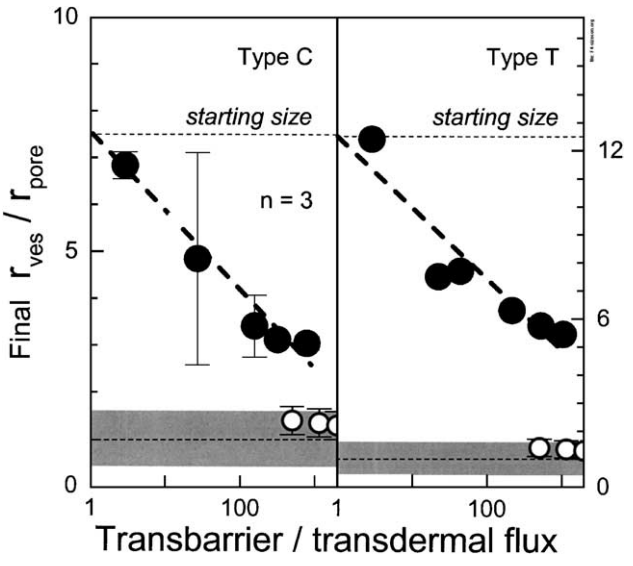

Fig. 3. Average final vesicle size relative to pore size as a function of suspension flux across a barrier. Two unrelated formulations (type C and T) give qualitatively similar results (bullets), distinctly different from those pertaining to liposomes (open circles, data from Ref. [27]. The flux is normalised relative to the transcutaneous flow of material measured in separate experiments. Grey zone gives an estimate for uncertainty limit of liposome and pore size, based on experience.

The ultradeformable mixed lipid vesicles were found to maintain their size during extrusion through a range of pores, including very narrow ones; Fig. 4 illustrates this.

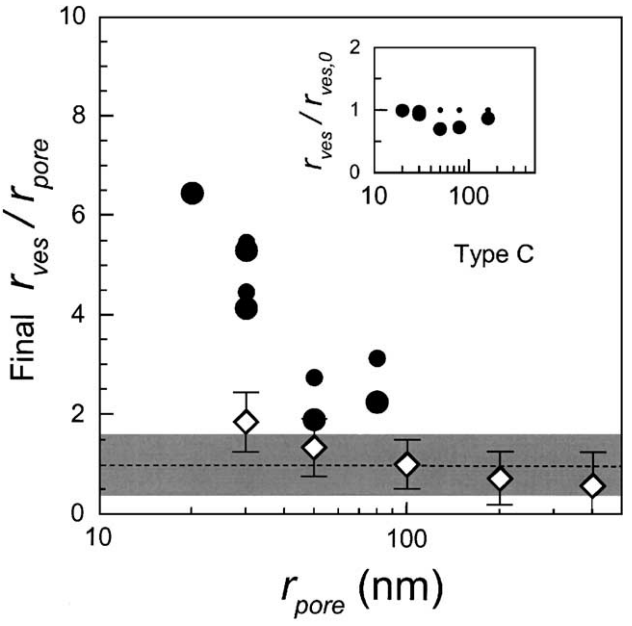

Fig. 4. Normalised vesicle size relatively to and as a function of pore diameter after the pressure-driven suspension transport through a semi-permeable barrier. Full, large symbols give results of measurements with ultradeformable vesicles, Transfersomes®; dots give the results extrapolated to small flux as shown in Fig. 3. Open symbols present the results for liposomes from Ref. [24]. Grey zone is defined in Fig. 3. Errors that do not show up are smaller than symbols.

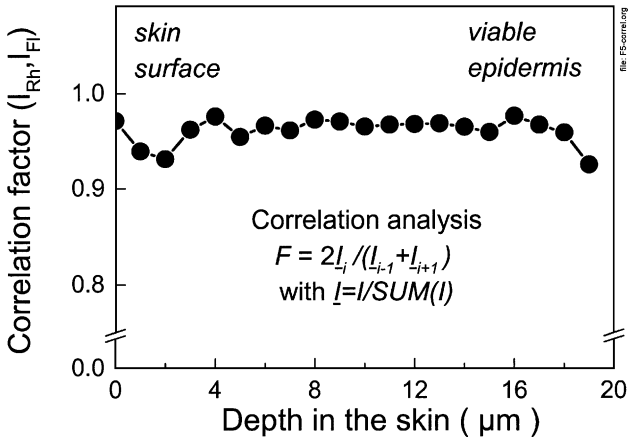

Fig. 5. One-dimensional correlation factor for the intradermal fluorescence of rhodamine-phosphatidylethanolamine (Rh-PE) and of fluorescein-phosphatidylethanolamine (Fl-PE) as a function of depth in murine skin treated with labelled ultradeformable vesicles, Transfersomes®, without occlusion.

The starting to final vesicle size ratio in the range tested is therefore close to one in all cases. Extrapolation into the low flux/pressure region (as explained for Fig. 3) even gives: $r_{ves}/r_{ves,0} = 1 \pm 0.05$ (see inset in Fig. 4). Extending the experimental range on the high end is problematic. This is due to the difficulty of preparing unilamellar vesicles with a starting size of two or more times greater than the pore diameter, which is the assay's lower sensitivity limit. This also explains why the r_{ves}/r_{pore} value in our data set approaches this lower limit.

3.2. Murine skin penetration

The resistance of ultradeformable vesicles to fragmentation in murine skin was studied *in vivo* using dual label fluorescence. The CLSM was used to monitor fluorophore distribution. The success of rhodamine-PE/fluorescein-PE co-labelled vesicle transport into the skin was deduced from the fluorescence intensity distribution profiles in the organ.

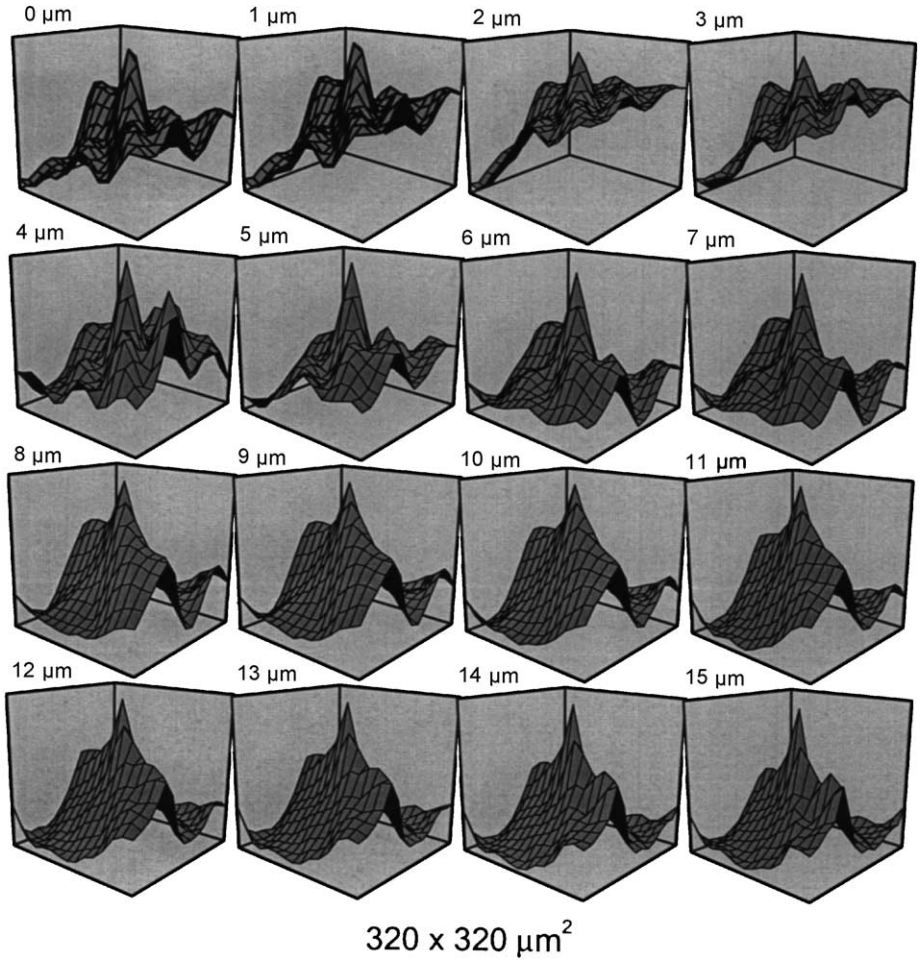

Fig. 6. Two-dimensional correlation analysis (Fourier representation) of lateral fluorescence intensity distribution in the skin treated non-occlusively with ultradeformable vesicles, Transfersomes®, co-labelled with rhodamine-phosphatidylethanolamine (Rh-PE) and fluorescein-phosphatidylethanolamine (Fl-PE). The central peak is indicative of similar spatial distributions of the two labels in the skin, and thus indirectly confirms chemical vesicle integrity during the skin passage. The size of each field is 320×320 µm^2.

The resolution limit of CLSM pictures is a combination of several factors: the different depth of focal planes associated with different analysed wavelengths, causing chromatic aberration; the relative distortion of pictures (e.g., due to astigmatism); and the focal resolution-limit of each individual microscopic picture. We considered all these factors when comparing the confocal micrographs to deduce the actual distribution of individual labels in the skin at different depths. Both labels were then concluded to have a qualitatively similar penetration characteristic in the skin (data not shown).

Quantitative comparison of fluorescence intensities is not trivial for a variety of reasons, such as photo-bleaching and quenching. The latter can reflect variations in the micro-environment of a fluorescent probe; changes in the local salt or oxygen concentration; pH differences, to which the used dye is sensitive, etc. In order to compare quantitatively the micrographs pertaining to the different used labels, we first analysed fluorescence data with the conventional correlation analysis. This yielded correlation coefficients that reflected the similarity of each optical cross-section for the chosen label. Minor differences in peak intensity notwithstanding, the normalised profiles were very similar and well correlated (see Fig. 5). Specifically, in the stratum corneum, where the vesicles are exposed to the greatest stress, the correlation coefficient for both labels was above 0.95. Lowest values were measured deep in the viable epidermis, however.

To eliminate further the bias from the label-specific intensity variations, we exploited spatial information in the individual label distributions in each optical cross-section. For this purpose, we included translational shifts of the micrographs measured with individual labels at one depth against each other:

$$\text{Correlation}(\underline{r})_i = < I_i^{\text{Fl-PE}}; I(\underline{r})_i^{\text{Rh-PE}} > ,$$

$I(\underline{r})$ is the shift of micrograph I by a lateral vector $\underline{r}$. This allowed direct comparison of the proximal areas in the skin.

We expected to get hints about individual label demixing and repartitioning in the skin after vesicles disintegration, if any occurred. Less quantitatively, we interpreted the central peak in the resulting two-dimensional correlation maps as a measure of the similarity in the spatial distribution of both inspected labels, according to the theory of Fourier analysis.

Results of our CLSM data analysis are given in Fig. 6. They confirm the basic similarity of the two-dimensional correlation function for both fluorescent labels to the depth of 15 μm in the skin; this is 5–8 μm below the stratum corneum/viable epidermis boundary in murine skin. More details on the skin penetration profiles of fluorescent ultra-deformable vesicles are given in Ref. [34].

The high level of correlation in the spatial distribution of different investigated labels in the skin barrier is not what would be expected if vesicles fell apart or if lipid aggregates exchanged their material extensively with the cells in the skin. At the depth of approx. 6 μm, where the skin permeability barrier is highest [34], one would expect maximum stress on vesicles penetrating intercellular contacts. If ultra-deformable vesicles in this region underwent complete disintegration, or were engaged in strong fragmentation, label demixing should be detected; the central correlation peak should then diminish, or even disappear. As the peak is preserved throughout the stratum corneum, this is an indication of the vesicle's resistance to said changes.

To substantiate the abovementioned conclusion, we examined the size of transdermally delivered Transfersomes® in the serum.

The elution profile of the sera collected from the mice treated with ultradeformable vesicles on the skin showed two main peaks. The first (fraction 6) was not observed with the control sera from the untreated mice; similar elution peak was seen in the chromatogram pertaining to the starting vesicle suspension, however. The second peak (fraction 13) was found in the blood of untreated and treated mice alike, but not with the original vesicle suspension. This maximum therefore corresponds to the fluorescent serum components.

It stands to reason that the first peak stems from the vesicles that have crossed the skin intact, and have subsequently found their way through lymphatic drainage into systemic blood circulation. The magnitude of such peaks can vary and depends on factors other than the average vesicle size. Averaging several chromatograms would therefore result in meaningless standard deviations. In Fig. 7, consequently, only the results of one experiment are given.

Confirmatory experiments were done with the fluorescence activated cell sorter. These experiments also revealed no difference between the sera spiked with the original vesicle suspension and the sera collected from the mice that

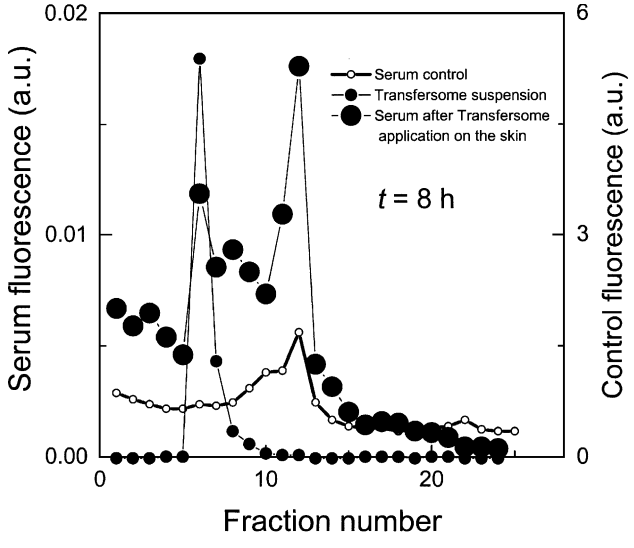

Fig. 7. Elution (size distribution) profile of the serum from untreated mice (dots) and from the mice treated with ultradeformable, fluorescently labelled Transfersomes® on non-occluded skin (bullets) for 8 h. The result of control measurement with the starting suspension is shown as open, small circles.

received ultradeformable vesicles on the skin (data not shown).

4. Discussion

To date, no general concept has been agreed upon to explain the fate of lipid vesicles on and in the skin. Different researchers have studied the fate of epicutaneously applied vesicles with electron microscopy [18], perturbed γ,γ angular correlation spectroscopy (PAC) [17], fluorescence spectroscopy [20], and other experimental methods [16]. Generally, only few [43,44], if any [18], vesicles were found in the skin. This was explained with the lack of vesicle transport into the organ, in agreement with our own results obtained with conventional lipid vesicles.

It is therefore clear that conventional vesicles are confined to the skin surface, with exception of pilosebaceous units [34,45] and rare skin packing imperfections (see Ref. [34] and unpublished data). An alternative explanation would be the lack of experimental sensitivity.

With the labelled ultradeformable vesicles we uncovered the existence of hydrophilic pathways in the skin [34]. These are typically located between cell envelopes and intercellular lipids and can be widened into 'virtual channels.' The resulting transcutaneous pathways can accommodate specially designed, highly deformable, and hydrophilic lipid aggregates. The proviso is that said aggregates are sensitive enough to the transdermal hydration gradient, so as to open channels in the skin barrier, and simultaneously are deformable enough to fit into channel openings. Obviously, even the most deformable vesicles cannot enter a significantly narrower pore without volume change; if the expansivity/compressibility of a vesicle bilayer is too small, pore entry is impossible.

Any vesicle therefore must lose some of its content during deformation in a pore (see Fig. 2). This compensates for the volume difference between a sphere and an ellipsoid, or any other non-spherical shape adapted to the pore size. In practice, such a volume exchange does not negatively affect trans-barrier transport of the vesicle associated agents. This holds true as long as volume exchange takes place inside a pore as the confined surrounding and the limited volume of extravesicular space prevent an escape of released content. Transient vesicle poration inside a narrow channel even offers an opportunity for additional loading of vesicle interior with water-soluble substances; this is likely to happen inside a transcutaneous channel during the hydrotaxis-driven transport. Vesicle post-loading is then driven by the outside–inside directed concentration gradient, caused by water evaporation from the skin surface.

Our experiments revealed that the final, relative vesicle size is a function of transport rate: with increasing trans-barrier flux the relative average aggregate size typically decreases, $\Delta r_{\mathrm{ves}} \equiv r_{\mathrm{ves,start}} - r_{\mathrm{ves,end}} \geq 0$. The process is quasi-exponential (see the curves in Fig. 3) with an essentially constant, and vesicle composition-independent, normalised decrement:

$$\Delta r_{\mathrm{ves,norm}}(f) \equiv (r_{\mathrm{ves,final}}(f) - r_{\mathrm{pore}})/(r_{\mathrm{ves,star}} - r_{\mathrm{pore}}) \propto \log f.$$

Vesicles fragmentation is thus appreciable only if flux is high. Little or no vesicle size diminution occurs at low barrier passage rate.

The results given in Fig. 3 show that high vesicles deformability allows even relatively large aggregates to maintain their average size during crossing a pore. Higher flow through a pore dissipates more energy, however. Work is now partly consumed to overcome viscous friction before and in the pore and partly for vesicle diminution. The fact that the change in diameter for vesicles of different composition and size is similar on a relative rather than on an absolute scale (cf. the last empirical mathematical relation given above) is *per se* revealing. It suggests that vesicles are fragmented in the turbulent stream of a fluid before a pore rather than in the pore proper.

Under all experimental conditions used in this work, the ultradeformable vesicles remained appreciably larger than the nominal pore size: $r_{\mathrm{v,final}}/r_{\mathrm{pore}} \sim 3\ldots6$. This is appreciable, taken that the tested pore width (20 nm) was two times smaller than the smallest reasonable diameter of a conventional phosphatidylcholine vesicle (45 nm) and 7–12 times smaller than the starting Transfersome® diameter. Ultradeformable vesicles thus must have survived correspondingly strong elongation in a pore (cf. Fig. 2). This must have involved at least local bilayer poration at vesicle end(s), allowing rapid expulsion of the excess water volumes. This reflects the fact that a sphere has a greater volume/surface ratio than a cylindrical vesicle. Deformed vesicles inside a pore therefore must have at least transiently open end(s) and can easily be mistaken for endogenous lipid multilamellae. One should not expect to find the customary spherical, closed vesicles in very narrow pores.

Extensive vesicle elongation in the vortex in front of a pore is more difficult to sustain than in the confined space of a pore. Pre-barrier vesicle elongation is thus prone to lead to progressive vesicle fragmentation with increasing trans-barrier flux and increasing turbulence in the stream of the pore-approaching fluid. Flux-effect is illustrated in Fig. 3 and corroborates the conclusion.

In principle, the vesicles fragmented before or in a pore could fuse back. The probability for this increases with vesicle concentration, but probably did not affect the outcome of our experiments. If it did, the pore size and flux dependences illustrated in Figs. 3 and 4 should be different. They should show discrete steps indicative of fusion or at least should yield a detectable proportion of anomalously large vesicles.

We estimated that the average width of pathways through the skin is 20–30 nm [32]. A different experimental method used; by other authors; yielded a similar value of 40 nm [14]. This is why we chose the pores in the skin surrogate

used in this study to have such diameter. The choice permitted us to assess directly vesicle diameter changes in the biologically relevant barriers for highly deformable mixed lipid vesicles and for conventional liposomes.

With the former kind of vesicles we observed only insignificant changes in lipid aggregate size when trans-barrier flux was similar to the rate of material flow through the skin. Even in the case of much higher suspension flux—and thus of very large shear- and turbulence-stress on a vesicle—the final size of ultradeformable vesicles was 3–6-fold greater than the nominal diameter of pores in a barrier. In contrast, liposomes were found to break down during trans-barrier passages when pores were at least two times smaller than the average vesicle diameter [15]; the proviso was that such lipid vesicles were pushed into pores with a pressure of at least one order of magnitude greater than in the tests with ultradeformable vesicles. This is consistent with the previous findings for liposomes by other authors [23–27]. The deviant behaviour of ultradeformable vesicles and liposomes thus provides a compelling evidence for the unique capability of the vesicles with a highly flexible bilayer to move through a semi-permeable barrier as intact, but dynamic, entities.

The high value of fluorescence distribution correlation factor (Fig. 5) and the persistence of the central peak in the two-dimensional correlation function for both labels tested (Fig. 6) have the same meaning. They jointly support the conclusion that chemical composition of the tested lipid vesicles, as reflected in the distribution of different labels in the skin, does not change appreciably during barrier passage. In case of significant fragmentation, which exposes bilayer edges with a different affinity for the two labels tested, such a change should be observed, however. It is not possible to perform a similar experiment with liposomes, since such vesicles do not penetrate the skin to an appreciable depth [15].

The outcome of vesicle size determination by the size-exclusion chromatography done before and after the skin penetration complements aforesaid findings. It furthermore extends the claim to physical (size) stability, that was demonstrated directly in experiments with the skin surrogate. Our size chromatography results do not exclude the possibility that some vesicles may have changed their size; in fact, one would expect this to happen in the bloodstream. Our results do show, however, that at least some lipid aggregates must have reached the circulation as relatively large entities, that is, intact.

We previously reported that radiolabelled phospholipids, incorporated into ultradeformable vesicles, are transported across the skin and reach systemic blood circulation via the lymph in appreciable quantity [15]. In principle, this could happen in the form of monomers/small fragments or of the preserved, more or less ‘intact’ vesicles. If the former scenario were true, one would expect lipids partitioning into lipoproteins in the serum and their circulation in the body. In the other extreme, the vesicle-derived material, which reaches the blood in the form of vesicles, should accumulate in the liver, as this organ is known to eliminate particulates from the body. This is seen, for example, after subcutaneous injections of conventional liposomes smaller than approximately 120 nm [46]; approximately 30% of the value achieved by an intravenous injection of such vesicles is detected in the liver after corresponding s.c. injection. An application of the radioactively labelled Transfersomes® on the skin leads to a similar biodistribution. Dependent on the applied dose, 5–30% of the epicutaneously administered label from the ultradeformable vesicles is found in the liver [32]. This also supports the view that Transfersomes® cross the skin barrier as vesicles rather than as bilayer fragments.

Biodistribution measurements can only give an indication of aggregate size after the skin crossing. To get a more quantitative picture, we separated fluorescent entities in the sera of the mice treated epicutaneously with a labelled vesicle suspension. This was done mainly with the size-exclusion chromatography, which is well established for the purpose [13], using epicutaneously Texas Red-DHPE labelled ultradeformable vesicles on the skin. Fluorescence elution profiles and refractive index traces were found to be similar to those measured with the serum blanks spiked with the original vesicle suspension (see Fig. 7). Fluorescence activated cell sorter pictures obtained with the corresponding samples were also undistinguishable (not shown). This proves that aggregate size has not changed detectably during the skin crossing.

In summary, we investigated the transport of various aggregates in the form of vesicles through a barrier with pores much smaller than the average vesicle diameter. We detected great disparity in the behaviour of highly deformable and conventional lipid vesicles. Most importantly, the former kind of vesicles can cross semi-permeable barriers essentially intact, whereas the latter type of lipid aggregates either cloggs or breaks at the barrier. The conditions for the former phenomenon are high lipid bilayer flexibility and permeability and minimum tearing stress on the vesicles. Similar conclusions are made for the artificial semi-permeable barriers and for the skin, which is a premier biological boundary.

Acknowledgements

We would like to thank Veronique Detappe for her contribution to flux measurements. We also wish to thank Dr. P. Hutzler (Institut für Pathologie, GSF, Neuherberg) and to Mrs. S. Möllenstädt (Institut für Strahlenbiologie, GSF, Neuherberg) for their support with the CLSM and animal work, respectively. The help of Dr. J. Dreher (Leibnitz Rechenzentrum, München) was important for the 3D visualization work.

References

[1] G. Vanlerberghe, R.M. Handjani-Vila, A. Ribier, Colloq. Nationaux C. N. R. S. (1978) 938–957.
[2] M. Mezei, V. Gulasekharam, Life Sci. 26 (1980) 1473–1477.

[3] A.Y. Ozer, A.A. Hincal, J.A. Bouwstra, Eur. J. Pharm. Biopharm. 37 (1991) 75–81.
[4] H.E.J. Hofland, R. Van der Geest, J.A. Bouwstra, H.E. Bodde, H.E. Junginger, Pharm. Res. 11 (1994) 659–664.
[5] A.J. Vermorken, M.W. Hukkelhoven, A.M. Vermeesch-Markslag, C.M. Goos, P. Wirtz, J. Ziegenmeyer, J. Pharm. Pharmacol. 36 (1984) 334–336.
[6] J. Lasch, W. Wohlrab, Biomed. Biochim. Acta 45 (1986) 1259–1295.
[7] N. Weiner, K. Egbaria, C. Ramachandran, in: O. Braun-Falco, H.C. Korting, H.I. Maibach (Eds.), Liposome Dermatics, Springer-Verlag, Berlin, 1992, pp. 242–250.
[8] J. du Plessis, K. Egbaria, C. Ramachandran, N. Weiner, Antiviral Res. 18 (1992) 259–265.
[9] Y. Takeuchi, H. Yasukawa, Y. Yamaoka, Y. Morimoto, S. Nakao, Y. Fukumori, T. Fukuda, Chem. Pharm. Bull. (Tokyo) 40 (1992) 484–487.
[10] N.B. Vutla, G.V. Betageri, A.K. Banga, J. Pharm. Sci. 85 (1996) 5–8.
[11] G. Cevc, Expert Opin. Invest. Drugs 6 (1997) 1887–1937.
[12] A. Meybeck, in: Liposome Dermatics, (O. Braun-Falco, H.C. Korting and H.I. Maibach, Eds.) Springer Verlag, Berlin, 1992, pp. 341–345.
[13] S. Lesieur, C. Grabielle-Madelmont, M.T. Paternostre, M. Olivon, Anal. Biochem. 192 (1991) 334–343.
[14] V. Aguiella, K. Kontturi, L. Murtomäki, P. Ramírez, J. Controlled Release 32 (1994) 249–257.
[15] G. Cevc, G. Blume, A. Schätzlein, D. Gebauer, A. Paul, Adv. Drug Delivery Rev. 418 (1996) 349–378.
[16] H. Schreier, J. Bouwstra, J. Controlled Release 30 (1994) 1–15.
[17] R. Schubert, M. Joos, M. Deicher, R. Magerle, J. Lasch, Biochim. Biophys. Acta 1150 (1993) 162–164.
[18] M.E. van Kuijk-Meuwissen, H.E. Junginger, J.A. Bouwstra, Biochim. Biophys. Acta 1371 (1998) 31–39.
[19] J. Lasch, R. Laub, W. Wohlrab, J. Controlled Release 18 (1992) 55–58.
[20] S. Zellmer, W. Pfeil, J. Lasch, Biochim. Biophys. Acta 1237 (1995) 176–182.
[21] S.M. Short, W. Rubas, B.D. Paasch, R.J. Mrsny, Pharm. Res. 12 (1995) 1140–1145.
[22] F. Olson, C.A. Hunt, F.C. Szoka, W.J. Vail, D. Papahadjopoulos, Biochim. Biophys. Acta 557 (1979) 9–23.
[23] M.J. Hope, M.B. Bally, G. Webb, P.R. Cullis, Biochim. Biophys. Acta 812 (1985) 55–65.
[24] L.D. Mayer, M.J. Hope, P.R. Cullis, Biochim. Biophys. Acta 856 (1986) 161–168.
[25] H. Jousma, H. Talsma, F. Spies, J.G.H. Joosten, H.E. Junginger, D.J.A. Crommelin, Int. J. Pharm. 35 (1987) 263–274.
[26] R. Nayer, M.J. Hope, P.R. Cullis, Biochim. Biophys. Acta 986 (1989) 200–206.
[27] D.G. Hunter, B.J. Frisken, Biophys. J. 74 (1998) 2996–3002.
[28] B.J. Frisken, C. Asman, P.J. Patty, Langmuir 16 (2000) 928–933.
[29] M.E.M.J. van Kuijk-Meuwissen, L. Mougin, H.E. Junginger, J.A. Bouwstra, J. Controlled Release 56 (1998) 189–196.
[30] G. Cevc, G. Blume, Biochim. Biophys. Acta 1514 (2001) 191–205.
[31] G. Cevc, in: R. Lipowsky (Ed.), Handbook of Physics of Biological Systems, vol. I, Elsevier, Amsterdam, 1995, pp. 441–466, Chapter 9.
[32] G. Cevc, Crit. Rev. Ther. Drug Carrier Syst. 13 (1996) 257–388.
[33] G. Cevc, G. Blume, Biochim. Biophys. Acta 1104 (1992) 226–232.
[34] A. Schätzlein, G. Cevc, Br. J. Dermatol. 1368 (1998) 201–215.
[35] G. Cevc, G. Blume, A. Schätzlein, J. Controlled Release 45 (1996) 211–226.
[36] G. Cevc, D. Gebauer, A. Schätzlein, G. Blume, J. Stieber, Biochim. Biophys. Acta 1368 (1998) 201–215.
[37] A. Paul, G. Cevc, B.K. Bachhawat, Eur. J. Immunol. 25 (1995) 3521–3524.
[38] A. Paul, G. Cevc, Vaccine Res. 4 (1995) 145–164.
[39] R.O. Potts, R.H. Guy, Pharm. Res. 9 (1992) 663–669.
[40] B.A. Cornell, G.C. Fletcher, J. Middlehurst, F. Separovic, Biochim. Biophys. Acta 690 (1982) 15–19.
[41] S.E. Schullery, C.F. Schmidt, P. Felgner, T.W. Tillack, T.E. Thompson, Biochemistry 19 (1980) 3919–3923.
[42] ASTM E 128-99, American society for testing and materials, West Conshohocken, PA, USA, 1999. 1–3.
[43] M. Foldvari, G.T. Faulkner, M. Mezei, J. Microencapsul. 5 (1988) 231–241.
[44] J.A. Bouwstra, P.L. Honeywell-Nguyen, A. de Graaff, W. Groenink, H.E. Junginger, Proceedings of 5th Int. Conf. 'Liposome Advances', London 17–21, Dec., 2001, pp. 51.
[45] A.C. Lauer, L.M. Lieb, C. Ramachandran, G. Flynn, N.D. Weiner, Pharm. Res. 12 (1995) 179–186.
[46] T.M. Allen, C.B. Hansen, L.S.S. Guo, Biochim. Biophys. Acta 1150 (1993) 9–16.